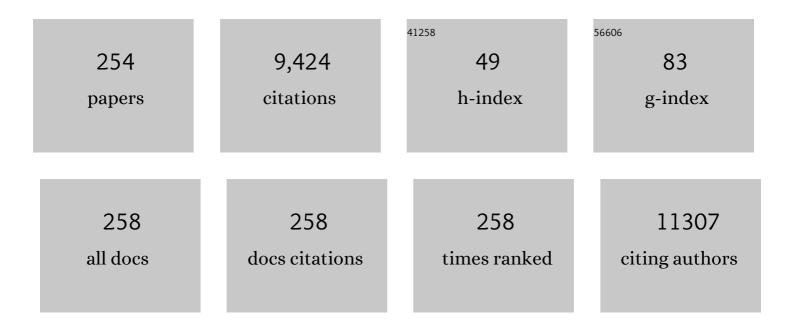
List of Publications by Year in descending order

Source: https://exaly.com/author-pdf/5569597/publications.pdf Version: 2024-02-01



PECIE COOL

#	Article	IF	CITATIONS
1	Mesoporous CuO/TiO2 catalysts prepared by the ammonia driven deposition precipitation method for CO preferential oxidation: Effect of metal loading. Fuel, 2022, 311, 122491.	3.4	12
2	ZnAl layered double hydroxide based catalysts (with Cu, Mn, Ti) used as noble metal-free three-way catalysts. Applied Clay Science, 2022, 217, 106390.	2.6	5
3	Efficient degradation and mineralization of diclofenac in water on ZnMe (Me: Al; Co; Ga) layered double hydroxides and derived mixed oxides as novel photocatalysts. Comptes Rendus Chimie, 2022, 25, 51-67.	0.2	0
4	Use of Nanoscale Carbon Layers on Ag-Based Gas Diffusion Electrodes to Promote CO Production. ACS Applied Nano Materials, 2022, 5, 7723-7732.	2.4	3
5	Atomic-scale detection of individual lead clusters confined in Linde Type A zeolites. Nanoscale, 2022, 14, 9323-9330.	2.8	2
6	Towards Highly Loaded and Finely Dispersed CuO Catalysts via ADP: Effect of the Alumina Support. Catalysts, 2022, 12, 628.	1.6	1
7	Binary icosahedral clusters of hard spheres in spherical confinement. Nature Physics, 2021, 17, 128-134.	6.5	42
8	Gold and Silver-Catalyzed Reductive Amination of Aromatic Carboxylic Acids to Benzylic Amines. ACS Catalysis, 2021, 11, 7672-7684.	5.5	18
9	Quantitative 3D real-space analysis of Laves phase supraparticles. Nature Communications, 2021, 12, 3980.	5.8	12
10	Mapping Composition–Selectivity Relationships of Supported Sub-10 nm Cu–Ag Nanocrystals for High-Rate CO ₂ Electroreduction. ACS Nano, 2021, 15, 14858-14872.	7.3	28
11	Development of monodisperse porous microspheres of MgAl-layered double hydroxide by droplet coagulation. Powder Technology, 2021, 391, 334-343.	2.1	5
12	A hyperbranched polymer synthetic strategy for the efficient fixation of metal species within nanoporous structures: Application in automotive catalysis. Chemical Engineering Journal, 2021, 421, 129496.	6.6	9
13	Layer-by-Layer-Stabilized Plasmonic Gold-Silver Nanoparticles on TiO2: Towards Stable Solar Active Photocatalysts. Nanomaterials, 2021, 11, 2624.	1.9	7
14	Interface Pattern Engineering in Core‧hell Upconverting Nanocrystals: Shedding Light on Critical Parameters and Consequences for the Photoluminescence Properties. Small, 2021, 17, e2104441.	5.2	17
15	Interface Pattern Engineering in Coreâ€Shell Upconverting Nanocrystals: Shedding Light on Critical Parameters and Consequences for the Photoluminescence Properties (Small 47/2021). Small, 2021, 17, 2170246.	5.2	0
16	In-depth structural characterization and magnetic properties of quaternary ferrite systems Co0.5Zn0.25M0.25Fe2O4 (MÂ= Ni, Cu, Mn, Mg). Journal of Alloys and Compounds, 2020, 816, 152674.	2.8	9
17	Bifunctional Nickel–Nitrogen-Doped-Carbon-Supported Copper Electrocatalyst for CO ₂ Reduction. Journal of Physical Chemistry C, 2020, 124, 1369-1381.	1.5	23
18	Ferrite@TiO2-nanocomposites as Z-scheme photocatalysts for CO2 conversion: Insight into the correlation of the Co-Zn metal composition and the catalytic activity. Journal of CO2 Utilization, 2020, 36, 177-186.	3.3	26

#	Article	IF	CITATIONS
19	Copper-Containing Mixed Metal Oxides (Al, Fe, Mn) for Application in Three-Way Catalysis. Catalysts, 2020, 10, 1344.	1.6	16
20	ZnTi layered double hydroxides as photocatalysts for salicylic acid degradation under visible light irradiation. Applied Clay Science, 2020, 197, 105757.	2.6	11
21	Fast Electron Tomography for Nanomaterials. Journal of Physical Chemistry C, 2020, 124, 27276-27286.	1.5	30
22	The Potential Use of Core-Shell Structured Spheres in a Packed-Bed DBD Plasma Reactor for CO2 Conversion. Catalysts, 2020, 10, 530.	1.6	9
23	Porphyrin functionalized bismuth ferrite for enhanced solar light photocatalysis. Dalton Transactions, 2020, 49, 8652-8660.	1.6	11
24	Plasmonic gold-embedded TiO2 thin films as photocatalytic self-cleaning coatings. Applied Catalysis B: Environmental, 2020, 267, 118654.	10.8	61
25	Harvesting solar light on a tandem of Pt or Pt-Ag nanoparticles on layered double hydroxides photocatalysts for p-nitrophenol degradation in water. Applied Clay Science, 2019, 182, 105250.	2.6	22
26	Design of Ti-Beta zeolites with high Ti loading and tuning of their hydrophobic/hydrophilic character. Microporous and Mesoporous Materials, 2019, 288, 109588.	2.2	23
27	Unraveling Structural Information of Turkevich Synthesized Plasmonic Gold–Silver Bimetallic Nanoparticles. Small, 2019, 15, e1902791.	5.2	33
28	Electron Transfer and Near-Field Mechanisms in Plasmonic Gold-Nanoparticle-Modified TiO ₂ Photocatalytic Systems. ACS Applied Nano Materials, 2019, 2, 4067-4074.	2.4	34
29	How process parameters and packing materials tune chemical equilibrium and kinetics in plasma-based CO2 conversion. Chemical Engineering Journal, 2019, 372, 1253-1264.	6.6	56
30	CuO/La0.5Sr0.5CoO3 nanocomposites in TWC. Applied Catalysis B: Environmental, 2019, 255, 117753.	10.8	19
31	Chemical and Structural Configuration of Pt-Doped Metal Oxide Thin Films Prepared by Atomic Layer Deposition. Chemistry of Materials, 2019, 31, 9673-9683.	3.2	8
32	Dynamic adsorption–desorption of methyl ethyl ketone on MCM-41 and SBA-15 decorated with thermally activated polymers. Journal of Industrial and Engineering Chemistry, 2019, 71, 465-480.	2.9	15
33	Template-free aqueous tape casting of hydrothermally synthesized barium titanate powder and the fabrication of highly {001}-{100} textured tapes. Ceramics International, 2018, 44, 9720-9727.	2.3	3
34	Characterization of silver-polymer core–shell nanoparticles using electron microscopy. Nanoscale, 2018, 10, 9186-9191.	2.8	11
35	Surface modified titanium dioxide using transition metals: nickel as a winning transition metal for solar light photocatalysis. Journal of Materials Chemistry A, 2018, 6, 9882-9892.	5.2	43
36	Inâ€Situ Synthesis of Bi ₂ O ₃ Nanoparticles on ZincMe (Me=Al or Cr) Layered Double Hydroxide Frameworks for Photocatalytic Oxygen Evolution from Water under Solar‣ight Activation. ChemCatChem, 2018, 10, 1598-1606.	1.8	4

#	Article	IF	CITATIONS
37	Novel magnetic nanocomposites containing quaternary ferrites systems Co0.5Zn0.25M0.25Fe2O4 (Mâ€=a€Ni, Cu, Mn, Mg) and TiO2-anatase phase as photocatalysts for wastewater remediation under solar light irradiation. Materials Science and Engineering B: Solid-State Materials for Advanced Technology, 2018, 230, 1-7.	1.7	48
38	A packed-bed DBD micro plasma reactor for CO2 dissociation: Does size matter?. Chemical Engineering Journal, 2018, 348, 557-568.	6.6	115
39	PGM-free CuO/LaCoO3 nanocomposites: New opportunities for TWC application. Applied Catalysis B: Environmental, 2018, 227, 446-458.	10.8	52
40	Preparation of CuO/SBA-15 catalyst by the modified ammonia driven deposition precipitation method with a high thermal stability and an efficient automotive CO and hydrocarbons conversion. Applied Catalysis B: Environmental, 2018, 223, 103-115.	10.8	30
41	Balancing nanotoxicity and returns in health applications: The Prisoner's Dilemma. Toxicology, 2018, 393, 83-89.	2.0	7
42	Insights into phosphate adsorption behavior on structurally modified ZnAl layered double hydroxides. Applied Clay Science, 2018, 165, 234-246.	2.6	82
43	Silver-polymer core-shell nanoparticles for ultrastable plasmon-enhanced photocatalysis. Applied Catalysis B: Environmental, 2017, 200, 31-38.	10.8	48
44	Automated discrete electron tomography– Towards routine high-fidelity reconstruction of nanomaterials. Ultramicroscopy, 2017, 175, 87-96.	0.8	27
45	Cu@LaNiO 3 based nanocomposites in TWC applications. Applied Catalysis B: Environmental, 2017, 209, 214-227.	10.8	39
46	Gas phase photocatalytic spiral reactor for fast and efficient pollutant degradation. Chemical Engineering Journal, 2017, 316, 850-856.	6.6	32
47	Catalytic activity of cobalt grafted on ordered mesoporous silica materials in N2O decomposition and CO oxidation. Molecular Catalysis, 2017, 437, 57-72.	1.0	13
48	Price tag in nanomaterials?. Journal of Nanoparticle Research, 2017, 19, 1.	0.8	19
49	Synthesis of L-serine modified benzene bridged periodic mesoporous organosilica and its catalytic performance towards aldol condensations. Microporous and Mesoporous Materials, 2017, 251, 1-8.	2.2	14
50	Mechanistic Insight into the Photocatalytic Working of Fluorinated Anatase {001} Nanosheets. Journal of Physical Chemistry C, 2017, 121, 26275-26286.	1.5	23
51	Plasmonic Near-Field Localization of Silver Core–Shell Nanoparticle Assemblies via Wet Chemistry Nanogap Engineering. ACS Applied Materials & Interfaces, 2017, 9, 41577-41585.	4.0	34
52	Tuning component enrichment in amino acid functionalized (organo)silicas. Catalysis Communications, 2017, 88, 85-89.	1.6	10
53	Molten-salt synthesis of tetragonal micron-sized barium titanate from a peroxo-hydroxide precursor. Advanced Powder Technology, 2017, 28, 146-154.	2.0	6
54	A framework for health-related nanomaterial grouping. Biochimica Et Biophysica Acta - General Subjects, 2017, 1861, 1478-1485.	1.1	5

#	Article	IF	CITATIONS
55	A Green Route to Copper Loaded Silica Nanoparticles Using Hyperbranched Poly(Ethylene Imine) as a Biomimetic Template: Application in Heterogeneous Catalysis. Catalysts, 2017, 7, 390.	1.6	8
56	Comparison between a Water-Based and a Solvent-Based Impregnation Method towards Dispersed CuO/SBA-15 Catalysts: Texture, Structure and Catalytic Performance in Automotive Exhaust Gas Abatement. Catalysts, 2016, 6, 164.	1.6	14
57	Synthesis of aluminum-containing hierarchical mesoporous materials with columnar mesopore ordering by evaporation induced self-assembly. Microporous and Mesoporous Materials, 2016, 234, 186-195.	2.2	7
58	Hyperbranched polyethyleneimine towards the development of homogeneous and highly porous CuO–CeO2–SiO2 catalytic materials. Chemical Engineering Journal, 2016, 300, 343-357.	6.6	14
59	Quaternary M0.25Cu0.25Mg0.5Fe2O4 (M=Ni, Zn, Co, Mn) ferrite oxides: Synthesis, characterization and magnetic properties. Materials Research Bulletin, 2016, 81, 63-70.	2.7	21
60	Hydrothermal synthesis and formation mechanism of tetragonal barium titanate in a highly concentrated alkaline solution. Ceramics International, 2016, 42, 10967-10975.	2.3	35
61	Post-synthesis bromination of benzene bridged PMO as a way to create a high potential hybrid material. Microporous and Mesoporous Materials, 2016, 236, 244-249.	2.2	9
62	Metal loaded nanoporous silicas with tailor-made properties through hyperbranched polymer assisted templating approaches. Microporous and Mesoporous Materials, 2016, 235, 107-119.	2.2	11
63	Plasmonic â€ ⁻ rainbow' photocatalyst with broadband solar light response for environmental applications. Applied Catalysis B: Environmental, 2016, 188, 147-153.	10.8	49
64	Texturing of hydrothermally synthesized BaTiO3 in a strong magnetic field by slip casting. Ceramics International, 2016, 42, 5382-5390.	2.3	14
65	Nano - patents and Literature Frequency as Statistical Innovation Indicator for the use of Nano - porous Material in Three Major Sectors: Medicine, Energy and Environment. Journal of Engineering Science and Technology Review, 2016, 9, 24-35.	0.2	5
66	Catalytic activity of rhodium grafted on ordered mesoporous silica materials modified with aluminum in N2O decomposition. Catalysis Today, 2015, 257, 51-58.	2.2	11
67	Novel method to synthesize highly ordered ethane-bridged PMOs under mild acidic conditions: Taking advantages of phosphoric acid. Microporous and Mesoporous Materials, 2015, 207, 61-70.	2.2	6
68	Hydrothermally synthesized BaTiO3 textured in a strong magnetic field. Ceramics International, 2015, 41, 5397-5402.	2.3	8
69	Photo-responsive behavior of γ-Fe2O3 NPs embedded into ZnAlFe-LDH matrices and their catalytic efficiency in wastewater remediation. Catalysis Today, 2015, 252, 7-13.	2.2	32
70	Asymmetric dyes align inside carbon nanotubes to yield a large nonlinear optical response. Nature Nanotechnology, 2015, 10, 248-252.	15.6	88
71	New insights into the mesophase transformation of ethane-bridged PMOs by the influence of different counterions under basic conditions. RSC Advances, 2015, 5, 5553-5562.	1.7	6
72	Self-Assembly of Pluronic F127—Silica Spherical Core–Shell Nanoparticles in Cubic Close-Packed Structures. Chemistry of Materials, 2015, 27, 5161-5169.	3.2	47

#	Article	IF	CITATIONS
73	Direct-synthesis method towards copper-containing periodic mesoporous organosilicas: detailed investigation of the copper distribution in the material. Dalton Transactions, 2015, 44, 9970-9979.	1.6	11
74	The ASTRA Toolbox: A platform for advanced algorithm development in electron tomography. Ultramicroscopy, 2015, 157, 35-47.	0.8	652
75	Glycerol-derived Mesoporous Carbon: N2-sorption and SAXS Data Evaluation. Materials Today: Proceedings, 2015, 2, 3836-3845.	0.9	4
76	ZnTiLDH and the Derived Mixed Oxides as Mesoporous Nanoarchitectonics with Photocatalytic Capabilities. Journal of Inorganic and Organometallic Polymers and Materials, 2015, 25, 259-266.	1.9	29
77	Photocatalytic removal of phenol and methylene-blue in aqueous media using TiO2@LDH clay nanocomposites. Catalysis Today, 2015, 252, 120-127.	2.2	107
78	LDH and TiO2/LDH-type nanocomposite systems: A systematic study on structural characteristics. Microporous and Mesoporous Materials, 2015, 203, 208-215.	2.2	47
79	Pore REconstruction and Segmentation (PORES) method for improved porosity quantification of nanoporous materials. Ultramicroscopy, 2015, 148, 10-19.	0.8	7
80	Fabrication of CeO2/LDHs self-assemblies with enhanced photocatalytic performance: A case study on ZnSn-LDH matrix. Applied Catalysis B: Environmental, 2015, 164, 251-260.	10.8	71
81	Assemblies of nanoparticles of CeO2–ZnTi-LDHs and their derived mixed oxides as novel photocatalytic systems for phenol degradation. Applied Catalysis B: Environmental, 2014, 150-151, 157-166.	10.8	99
82	Iron exchanged ZSM-5 and Y zeolites calcined at different temperatures: activity in N2O decomposition. Journal of Porous Materials, 2014, 21, 91-98.	1.3	23
83	Zeolite β nanoparticles based bimodal structures: Mechanism and tuning of the porosity and zeolitic properties. Microporous and Mesoporous Materials, 2014, 185, 204-212.	2.2	12
84	Catalytic decomposition and reduction of N2O over micro-mesoporous materials containing Beta zeolite nanoparticles. Applied Catalysis B: Environmental, 2014, 146, 112-122.	10.8	50
85	In situ IR spectroscopic study to reveal the impact of the synthesis conditions of zeolite Î ² nanoparticles on the acidic properties of the resulting zeolite. Chemical Engineering Journal, 2014, 237, 372-379.	6.6	39
86	Probing framework–guest interactions in phenylene-bridged periodic mesoporous organosilica using spin-probe EPR. Physical Chemistry Chemical Physics, 2014, 16, 22623-22631.	1.3	11
87	Threeâ€Dimensional Characterization of Nobleâ€Metal Nanoparticles and their Assemblies by Electron Tomography. Angewandte Chemie - International Edition, 2014, 53, 10600-10610.	7.2	59
88	Atomic layer deposition-based tuning of the pore size in mesoporous thin films studied by in situ grazing incidence small angle X-ray scattering. Nanoscale, 2014, 6, 14991-14998.	2.8	44
89	Synthesis and Characterization of Photoreactive TiO ₂ –Carbon Nanosheet Composites. Journal of Physical Chemistry C, 2014, 118, 21031-21037.	1.5	8
90	Demonstrating the Benefits and Pitfalls of Various Acidity Characterization Techniques by a Case Study on Bimodal Aluminosilicates. Langmuir, 2014, 30, 1880-1887.	1.6	12

#	Article	IF	CITATIONS
91	Pt-doped semiconductive oxides loaded on mesoporous SBA-15 for gas sensing. Comptes Rendus Chimie, 2014, 17, 717-724.	0.2	12
92	Photocatalytic acetaldehyde oxidation in air using spacious TiO2 films prepared by atomic layer deposition on supported carbonaceous sacrificial templates. Applied Catalysis B: Environmental, 2014, 160-161, 204-210.	10.8	37
93	Synthesis and characterization of catalytic metal semiconductor-doped siliceous materials with ordered structure for chemical sensoring. Journal of Porous Materials, 2013, 20, 1119-1128.	1.3	2
94	Effects of copper and vanadium deposition in multi-walled hydrogen trititanate and mixed-phase anatase/trititanate nanotubes. Dalton Transactions, 2013, 42, 12148.	1.6	2
95	Mg–Al and Zn–Fe layered double hydroxides used for organic species storage and controlled release. Materials Science and Engineering C, 2013, 33, 5071-5078.	3.8	22
96	The influence of the Ti4+ location on the formation of self-assembled nanocomposite systems based on TiO2 and Mg/Al-LDHs with photocatalytic properties. Applied Catalysis B: Environmental, 2013, 134-135, 274-285.	10.8	56
97	Hierarchical materials originated from mesoporous MCF material and Beta zeolite nanoparticles – synthesis and catalytic activity in N2O decomposition. Journal of the Chinese Advanced Materials Society, 2013, 1, 48-55.	0.7	3
98	Synthesis of uniformly dispersed anatase nanoparticles inside mesoporous silica thin films via controlled breakup and crystallization of amorphous TiO2 deposited using atomic layer deposition. Nanoscale, 2013, 5, 5001.	2.8	23
99	Investigation on the Low-Temperature Transformations of Poly(furfuryl alcohol) Deposited on MCM-41. Langmuir, 2013, 29, 3045-3053.	1.6	23
100	Hydrothermal synthesis of a concentrated and stable dispersion of TiO2 nanoparticles. Chemical Engineering Journal, 2013, 223, 135-144.	6.6	31
101	Controlling pore size and uniformity of mesoporous titania by early stage low temperature stabilization. Journal of Colloid and Interface Science, 2013, 391, 36-44.	5.0	15
102	Influence of Synthesis Conditions on Properties of Ethane-Bridged Periodic Mesoporous Organosilica Materials as Revealed by Spin-Probe EPR. Journal of Physical Chemistry C, 2013, 117, 22723-22731.	1.5	9
103	Microvolume TOC Analysis as Useful Tool in the Evaluation of Lab Scale Photocatalytic Processes. Catalysts, 2013, 3, 74-87.	1.6	6
104	Thermal transformation of polyacrylonitrile deposited on SBA-15 type silica. Journal of Thermal Analysis and Calorimetry, 2012, 110, 119-125.	2.0	35
105	New nano-architectures of mesoporous silica spheres analyzed by advanced electron microscopy. Nanoscale, 2012, 4, 1722.	2.8	4
106	Layered double hydroxides reconstructed in calcium glutamate aqueous solution as a complex delivery system. Applied Clay Science, 2012, 65-66, 37-42.	2.6	10
107	Is their potential for post-synthetic brominating reactions on benzene bridged PMOs?. Microporous and Mesoporous Materials, 2012, 164, 49-55.	2.2	5
108	New Operando IR Technique to Study the Photocatalytic Activity and Selectivity of TiO ₂ Nanotubes in Air Purification: Influence of Temperature, UV Intensity, and VOC Concentration. Journal of Physical Chemistry C, 2012, 116, 13252-13263.	1.5	62

#	Article	IF	CITATIONS
109	Experimental and statistical modeling study of low coverage gas adsorption of light alkanes on meso-microporous silica. Chemical Engineering Journal, 2012, 179, 52-62.	6.6	10
110	Hydrothermal synthesis of carbonate-free submicron-sized barium titanate from an amorphous precursor: Synthesis and characterization. Ceramics International, 2012, 38, 619-625.	2.3	13
111	The impact of framework organic functional groups on the hydrophobicity and overall stability of mesoporous silica materials. Materials Chemistry and Physics, 2012, 132, 1077-1088.	2.0	20
112	Preparation of barium titanate powders and colloidal processing in a strong (9.4T) magnetic field. Materials Letters, 2012, 67, 154-157.	1.3	9
113	A short solid-state synthesis leading to titanate compounds with porous structure and nanosheet morphology. Microporous and Mesoporous Materials, 2012, 147, 53-58.	2.2	13
114	Systematic evaluation of thermal and mechanical stability of different commercial and synthetic photocatalysts in relation to their photocatalytic activity. Microporous and Mesoporous Materials, 2012, 156, 62-72.	2.2	9
115	Formation of a Ti-siliceous trimodal material with macroholes, mesopores and zeolitic features via a one-pot templating synthesis. Journal of Porous Materials, 2012, 19, 153-160.	1.3	3
116	Immersion Calorimetry as a Tool To Evaluate the Catalytic Performance of Titanosilicate Materials in the Epoxidation of Cyclohexene. Langmuir, 2011, 27, 3618-3625.	1.6	26
117	Unraveling the Photocatalytic Activity of Multiwalled Hydrogen Trititanate and Mixed-Phase Anatase/Trititanate Nanotubes: A Combined Catalytic and EPR Study. Journal of Physical Chemistry C, 2011, 115, 2302-2313.	1.5	22
118	Synthesis and catalytic applications of combined zeolitic/mesoporous materials. Beilstein Journal of Nanotechnology, 2011, 2, 785-801.	1.5	44
119	Influence of Surfactant Concentration on the Surface Morphology of Hollow Silica Microspheres and Its Explanation. Microscopy and Microanalysis, 2011, 17, 766-771.	0.2	6
120	Influence of ammonia concentration on the formation of hollow silica microspheres via polystyrene beads templating. International Journal of Materials Research, 2011, 102, 1488-1492.	0.1	4
121	Removal of methyl–ethyl ketone vapour on polyacrylonitrile-derived carbon/mesoporous silica nanocomposite adsorbents. Microporous and Mesoporous Materials, 2011, 145, 65-73.	2.2	17
122	Mechanistic study of hydrocarbon formation in photocatalytic CO2 reduction over Ti-SBA-15. Journal of Catalysis, 2011, 284, 1-8.	3.1	118
123	The benefit of glass bead supports for efficient gas phase photocatalysis: Case study of a commercial and a synthesised photocatalyst. Chemical Engineering Journal, 2011, 174, 318-325.	6.6	55
124	Smart heating profiles for the synthesis of benzene bridged periodic mesoporous organosilicas. Chemical Engineering Journal, 2011, 175, 585-591.	6.6	6
125	SBA-15 mesoporous silica modified with rhodium by MDD method and its catalytic role for N2O decomposition reaction. Journal of Porous Materials, 2011, 18, 483-491.	1.3	30
126	Integrating efficient filtration and visible-light photocatalysis by loading Ag-doped zeolite Y particles on filtration membrane of alumina nanofibers. Journal of Membrane Science, 2011, 375, 69-74.	4.1	27

#	Article	IF	CITATIONS
127	New Insights in the Formation of Combined Zeolitic/Mesoporous Materials by using a Oneâ€Pot Templating Synthesis. European Journal of Inorganic Chemistry, 2011, 2011, 4234-4240.	1.0	14
128	Olefin isomerization reactions catalyzed by ruthenium hydrides bearing Schiff base ligands. Applied Organometallic Chemistry, 2011, 25, 601-607.	1.7	11
129	Influence of silica forming media on the synthesis of hollow silica microspheres. Microporous and Mesoporous Materials, 2011, 138, 17-21.	2.2	5
130	ZnO nanoparticles supported on mesoporous MCM-41 and SBA-15: a comparative physicochemical and photocatalytic study. Journal of Materials Science, 2010, 45, 5786-5794.	1.7	76
131	Threeâ€Dimensional Characterization of Helical Silver Nanochains Mediated by Protein Assemblies. Advanced Materials, 2010, 22, 2193-2197.	11.1	59
132	SBA-15 mesoporous silica modified with metal oxides by MDD method in the role of DeNOx catalysts. Microporous and Mesoporous Materials, 2010, 127, 133-141.	2.2	54
133	Textural property tuning of ordered mesoporous carbon obtained by glycerol conversion using SBA-15 silica as template. Carbon, 2010, 48, 1609-1618.	5.4	61
134	New TiO ₂ /MgAl-LDH Nanocomposites for the Photocatalytic Degradation of Dyes. Journal of Nanoscience and Nanotechnology, 2010, 10, 8227-8233.	0.9	31
135	Three-Dimensional Analysis of Carbon Nanotube Networks in Interconnects by Electron Tomography without Missing Wedge Artifacts. Microscopy and Microanalysis, 2010, 16, 210-217.	0.2	47
136	The use of small volume TOC analysis as complementary, indispensable tool in the evaluation of photocatalysts at lab-scale. Studies in Surface Science and Catalysis, 2010, 175, 321-324.	1.5	1
137	Self-Assembly and Diffusion of Block Copolymer Templates in SBA-15 Nanochannels. Journal of Physical Chemistry B, 2010, 114, 4223-4229.	1.2	21
138	Accessibility and Dispersion of Vanadyl Sites of Vanadium Silicate-1 Nanoparticles Deposited in SBA-15. Journal of Physical Chemistry C, 2010, 114, 12966-12975.	1.5	12
139	Benefit of Microscopic Diffusion Measurement for the Characterization of Nanoporous Materials. Chemical Engineering and Technology, 2009, 32, 1494-1511.	0.9	28
140	A scanning electron microscopy study on hollow silica microspheres: defects and influences of the synthesis composition. Journal of Sol-Gel Science and Technology, 2009, 49, 373-379.	1.1	0
141	Synthesis, structural characterization and photocatalytic activity of Ti-MCM-41 mesoporous molecular sieves. Journal of Porous Materials, 2009, 16, 109-118.	1.3	13
142	Synthesis and structural investigations on aluminium-free Ti-Beta/SBA-15 composite. Microporous and Mesoporous Materials, 2009, 117, 458-465.	2.2	26
143	Verified syntheses of mesoporous materials. Microporous and Mesoporous Materials, 2009, 125, 170-223.	2.2	575
144	Formation of a combined micro- and mesoporous material using zeolite Beta nanoparticles. Microporous and Mesoporous Materials, 2009, 120, 29-34.	2.2	49

#	Article	IF	CITATIONS
145	Optimisation of the surface properties of SBA-15 mesoporous silica for in-situ nanoparticle synthesis. Microporous and Mesoporous Materials, 2009, 120, 2-6.	2.2	6
146	Combined TiO2/SiO2 mesoporous photocatalysts with location and phase controllable TiO2 nanoparticles. Applied Catalysis B: Environmental, 2009, 88, 515-524.	10.8	70
147	Quantitative Three-Dimensional Modeling of Zeotile Through Discrete Electron Tomography. Journal of the American Chemical Society, 2009, 131, 4769-4773.	6.6	66
148	Is There Any Microporosity in Ordered Mesoporous Silicas?. Langmuir, 2009, 25, 939-943.	1.6	55
149	Rapid microwave-assisted synthesis of benzene bridged periodic mesoporous organosilicas. Journal of Materials Chemistry, 2009, 19, 3042.	6.7	20
150	Direct spectroscopic detection of framework-incorporated vanadium in mesoporous silica materials. Physical Chemistry Chemical Physics, 2009, 11, 5823.	1.3	23
151	The influence of the cationic ratio on the incorporation of Ti4+ in the brucite-like sheets of layered double hydroxides. Microporous and Mesoporous Materials, 2008, 111, 12-17.	2.2	43
152	Mesoporous material formed by acidic hydrothermal assembly of silicalite-1 precursor nanoparticles in the absence of meso-templates. Microporous and Mesoporous Materials, 2008, 110, 77-85.	2.2	23
153	Influence of the synthesis parameters of TiO2–SBA-15 materials on the adsorption and photodegradation of rhodamine-6G. Microporous and Mesoporous Materials, 2008, 110, 100-110.	2.2	56
154	Development of photocatalytic efficient Ti-based nanotubes and nanoribbons by conventional and microwave assisted synthesis strategies. Microporous and Mesoporous Materials, 2008, 114, 401-409.	2.2	55
155	Multi-step loading of titania on mesoporous silica: Influence of the morphology and the porosity on the catalytic degradation of aqueous pollutants and VOCs. Applied Catalysis B: Environmental, 2008, 84, 125-132.	10.8	34
156	SnIV-containing layered double hydroxides as precursors for nano-sized ZnO/SnO2 photocatalysts. Applied Catalysis B: Environmental, 2008, 84, 699-705.	10.8	84
157	Zn–Al layered double hydroxides: Synthesis, characterization and photocatalytic application. Microporous and Mesoporous Materials, 2008, 113, 296-304.	2.2	210
158	The merging of silica-surfactant microspheres under hydrothermal conditions. Microporous and Mesoporous Materials, 2008, 116, 141-146.	2.2	8
159	Photocatalytic study of P25 and mesoporous titania in aqueous and gaseous environment. Catalysis Communications, 2008, 9, 1787-1792.	1.6	11
160	Preparation of hollow silica spheres with different mesostructures. Journal of Non-Crystalline Solids, 2008, 354, 826-830.	1.5	23
161	A simple way to design highly active titania / mesoporous silica photocatalysts. Studies in Surface Science and Catalysis, 2008, 174, 377-380.	1.5	5
162	Deposition of Ti-modified aluminium-free zeolite Beta on SBA-15. Studies in Surface Science and Catalysis, 2008, , 217-220.	1.5	0

#	Article	lF	CITATIONS
163	Multistep Loading of Titania Nanoparticles in the Mesopores of SBA-15 for Enhanced Photocatalytic Activity. Journal of Nanoscience and Nanotechnology, 2007, 7, 2511-2515.	0.9	12
164	A facile synthesis of MCM-41 by ultrasound irradiation. Studies in Surface Science and Catalysis, 2007, 165, 169-172.	1.5	1
165	Growth of anatase nanoparticles inside the mesopores of SBA-15 for photocatalytic applications. Catalysis Communications, 2007, 8, 527-530.	1.6	13
166	Fast fabrication of hollow silica spheres with thermally stable nanoporous shells. Microporous and Mesoporous Materials, 2007, 98, 41-46.	2.2	36
167	Synthesis of siliceous materials with micro- and mesoporosity. Microporous and Mesoporous Materials, 2007, 104, 26-38.	2.2	89
168	Stabilisation of mesoporous TiO2 by different bases influencing the photocatalytic activity. Microporous and Mesoporous Materials, 2007, 99, 112-117.	2.2	47
169	Deposition of vanadium silicalite-1 nanoparticles on SBA-15 materials. Structural and transport characteristics of SBA-VS-15. Microporous and Mesoporous Materials, 2007, 99, 14-22.	2.2	23
170	Epoxidation of propylene with nitrous oxide on Rb2SO4-modified iron oxide on silica catalysts. Journal of Catalysis, 2007, 247, 86-100.	3.1	40
171	Quantitative Three-Dimensional Reconstruction of Catalyst Particles for Bamboo-like Carbon Nanotubes. Nano Letters, 2007, 7, 3669-3674.	4.5	88
172	Formation of spheres and siliceous plugs in synthesizing MCF materials. Journal of Porous Materials, 2007, 14, 417-421.	1.3	1
173	Selective catalytic reduction of NO with ammonia over porous clay heterostructures modified with copper and iron species. Catalysis Today, 2007, 119, 181-186.	2.2	51
174	Preparation and Characterization of Vanadium Oxide Deposited on Thermally Stable Mesoporous Titania. Journal of Physical Chemistry B, 2006, 110, 948-955.	1.2	33
175	Vanadium Silicalite-1 Nanoparticles Deposition onto the Mesoporous Walls of SBA-15. Mechanistic Insights from a Combined EPR and Raman Study. Journal of the American Chemical Society, 2006, 128, 8955-8963.	6.6	33
176	Investigation of the Morphology of the Mesoporous SBA-16 and SBA-15 Materials. Journal of Physical Chemistry B, 2006, 110, 9183-9187.	1.2	150
177	Selective catalytic oxidation of ammonia into nitrogen over PCH modified with copper and iron species. Catalysis Today, 2006, 114, 319-325.	2.2	51
178	Characteristics of new composite- and classical potentiometric sensors for the determination of pharmaceutical drugs. Electrochimica Acta, 2006, 51, 5062-5069.	2.6	18
179	Formation mechanism of SBA-16 spheres and control of their dimensions. Microporous and Mesoporous Materials, 2006, 93, 119-124.	2.2	41
180	Influence of the MCM-41 morphology on the vanadia deposition by a molecular designed dispersion method. Microporous and Mesoporous Materials, 2006, 95, 31-38.	2.2	19

#	Article	IF	CITATIONS
181	Structural features and photocatalytic behaviour of titania deposited within the pores of SBA-15. Applied Catalysis A: General, 2006, 312, 153-164.	2.2	60
182	Quantification of crystalline and amorphous content in porous samples from electron energy loss spectroscopy. Ultramicroscopy, 2006, 106, 630-635.	0.8	86
183	VOx supported SBA-15 catalysts for the oxidative dehydrogenation of ethylbenzene to styrene in the presence of N2O. Catalysis Today, 2006, 114, 307-313.	2.2	51
184	Catalytic performance of various mesoporous silicas modified with copper or iron oxides introduced by different ways in the selective reduction of NO by ammonia. Applied Catalysis B: Environmental, 2006, 62, 369-380.	10.8	138
185	Further investigations on the modified Stöber method for spherical MCM-41. Materials Chemistry and Physics, 2006, 97, 203-206.	2.0	30
186	The influence of temperature on the structural behaviour of sodium tri- and hexa-titanates and their protonated forms. Journal of Solid State Chemistry, 2005, 178, 1614-1619.	1.4	126
187	Influence of the initial iron concentration on the iron-loading in MCM-41 and thermal decomposition of the supported iron complexes. Microporous and Mesoporous Materials, 2005, 79, 299-305.	2.2	13
188	Diffusion effects in SBA-15 and its plugged analogous by a deposition of metal–acetylacetonate complexes. Microporous and Mesoporous Materials, 2005, 85, 119-128.	2.2	25
189	Preparation and characterization of SnO2 nanoparticles of enhanced thermal stability: The effect of phosphoric acid treatment on SnO2·nH2O. Colloids and Surfaces A: Physicochemical and Engineering Aspects, 2005, 268, 147-154.	2.3	68
190	Characterisation and reactivity of vanadia–titania supported SBA-15 in the SCR of NO with ammonia. Applied Catalysis B: Environmental, 2005, 61, 69-78.	10.8	48
191	Nitrous Oxide Reduction with Ammonia and Methane Over Mesoporous Silica Materials Modified with Transition Metal Oxides. Journal of Porous Materials, 2005, 12, 183-191.	1.3	16
192	Octane Hydroisomerization Over Hexagonal Mesoporous Aluminosilicates Synthesized from Leached Saponite. Journal of Porous Materials, 2005, 12, 35-40.	1.3	0
193	Morphology Variations of Plugged Hexagonal Templated Silica. Journal of Porous Materials, 2005, 12, 65-69.	1.3	26
194	Complementary use of Fourier transform laser microprobe mass spectrometry and time-of-flight static secondary ion mass spectrometry for the study of the surface adsorption of organic dyes on silicate materials. Rapid Communications in Mass Spectrometry, 2005, 19, 2809-2818.	0.7	4
195	Molecular designed vanadia–titania supported SBA-15 for the oxidative dehydrogenation of isobutane and propane. Studies in Surface Science and Catalysis, 2005, 156, 733-740.	1.5	1
196	Dehydrogenation of Ethylbenzene with Nitrous Oxide in the Presence of Mesoporous Silica Materials Modified with Transition Metal Oxides. Journal of Physical Chemistry A, 2005, 109, 330-336.	1.1	34
197	Characterization of Vanadium and Titanium Oxide Supported SBA-15. Journal of Physical Chemistry B, 2005, 109, 12071-12079.	1.2	54
198	Anatase Formation during the Synthesis of Mesoporous Titania and Its Photocatalytic Effect. Journal of Physical Chemistry B, 2005, 109, 10081-10086.	1.2	88

#	Article	IF	CITATIONS
199	Using mesoporous silica materials to immobilise biocatalysis-enzymes. Catalysis Communications, 2005, 6, 307-311.	1.6	80
200	Immobilisation behaviour of biomolecules in mesoporous silica materials. Catalysis Communications, 2005, 6, 591-595.	1.6	23
201	Adsorption of Hydrocarbons on Mesoporous SBA-15 and PHTS Materials. Langmuir, 2005, 21, 2447-2453.	1.6	41
202	Modification of MCM-48-, SBA-15-, MCF-, and MSU-type Mesoporous Silicas with Transition Metal Oxides Using the Molecular Designed Dispersion Method. Journal of Physical Chemistry B, 2005, 109, 11552-11558.	1.2	83
203	Catalytic Activity of MCM-48-, SBA-15-, MCF-, and MSU-Type Mesoporous Silicas Modified with Fe3+ Species in the Oxidative Dehydrogenation of Ethylbenzene in the Presence of N2O. Journal of Physical Chemistry A, 2005, 109, 9808-9815.	1.1	27
204	Deriving pore size distributions of solids with both micro- and mesopores from comparison plots. Studies in Surface Science and Catalysis, 2004, 154, 1456-1463.	1.5	0
205	Structure and microstructure of nanoscale mesoporous silica spheres. Solid State Sciences, 2004, 6, 489-498.	1.5	49
206	Effects of Strontium on the Physicochemical Characteristics of Hydroxyapatite. Calcified Tissue International, 2004, 75, 405-415.	1.5	89
207	Physicochemical and Structural Characterization of Mesoporous Aluminosilicates Synthesized from Leached Saponite with Additional Aluminum Incorporation ChemInform, 2004, 35, no.	0.1	Ο
208	Magnetism of iron-containing MCM-41 spheres. Journal of Magnetism and Magnetic Materials, 2004, 280, 31-36.	1.0	33
209	Design and applications of a home-built in situ FT-Raman spectroscopic cell. Spectrochimica Acta - Part A: Molecular and Biomolecular Spectroscopy, 2004, 60, 2969-2975.	2.0	10
210	Post-synthesis deposition of V-zeolitic nanoparticles in SBA-15. Chemical Communications, 2004, , 898.	2.2	20
211	Aluminum Incorporation into MCM-48 toward the Creation of BrÃ,nsted Acidity. Journal of Physical Chemistry B, 2004, 108, 13905-13912.	1.2	13
212	Quantitative Information on Pore Size Distribution from the Tangents of Comparison Plots. Langmuir, 2004, 20, 10115-10122.	1.6	16
213	Plugged Hexagonal Templated Silica (PHTS):Â An In-Depth Study of the Structural Characteristics. Journal of Physical Chemistry B, 2004, 108, 5263-5268.	1.2	57
214	Structural Investigation of Vanadyl-Acetylacetonate-Containing Precursors of TiOxâ^'VOxMixed Oxides on SBA-15. Journal of Physical Chemistry B, 2004, 108, 19404-19412.	1.2	20
215	Influence of polymer matrix and adsorption onto silica materials on the migration ofα-tocopherol into 95% ethanol from active packaging. Food Additives and Contaminants, 2004, 21, 1125-1136.	2.0	43
216	TiOx-VOxMixed Oxides on SBA-15 Support Prepared by the Designed Dispersion of Acetylacetonate Complexes:Â Spectroscopic Study of the Reaction Mechanisms. Journal of Physical Chemistry B, 2004, 108, 3794-3800.	1.2	31

#	Article	IF	CITATIONS
217	Novel strategies towards mesoporous titania and titania-silicate composites. Studies in Surface Science and Catalysis, 2004, 154, 789-796.	1.5	7
218	Surfactant-Directed Synthesis of Mesoporous Titania with Nanocrystalline Anatase Walls and Remarkable Thermal Stability. Journal of Physical Chemistry B, 2004, 108, 3713-3721.	1.2	100
219	Pillared Clays and Porous Clay Heterostructures. , 2004, , .		3
220	Characterization of the Acidic Properties of Mesoporous Aluminosilicates Synthesized from Leached Saponite with Additional Aluminum Incorporation ChemInform, 2003, 34, no.	0.1	0
221	Mesoporous templated silicates: an overview of their synthesis, catalytic activation and evaluation of the stability. Advances in Colloid and Interface Science, 2003, 103, 121-147.	7.0	179
222	The Influence of the Alcohol Concentration on the Structural Ordering of Mesoporous Silica:Â Cosurfactant versus Cosolvent. Journal of Physical Chemistry B, 2003, 107, 10405-10411.	1.2	145
223	A new strategy towards ultra stable mesoporous titania with nanosized anatase walls. Chemical Communications, 2003, , 1178-1179.	2.2	50
224	Characterization of the Acidic Properties of Mesoporous Aluminosilicates Synthesized from Leached Saponite with Additional Aluminum Incorporation. Journal of Physical Chemistry B, 2003, 107, 8599-8606.	1.2	15
225	Physicochemical and Structural Characterization of Mesoporous Aluminosilicates Synthesized from Leached Saponite with Additional Aluminum Incorporation. Chemistry of Materials, 2003, 15, 4863-4873.	3.2	15
226	Controlled formation of amine-templated mesostructured zirconia with remarkably high thermal stability. Journal of Materials Chemistry, 2003, 13, 3033.	6.7	33
227	Controlled Reduction of the Acid Site Density of SAPO-34 Molecular Sieve by Means of Silanation and Disilanation. Journal of Physical Chemistry B, 2003, 107, 3161-3167.	1.2	26
228	Structure of nanoscale mesoporous silica spheres?. Journal of Physics Condensed Matter, 2003, 15, S3037-S3046.	0.7	30
229	Leached Natural Saponite as the Silicate Source in the Synthesis of Aluminosilicate Hexagonal Mesoporous Materials. Journal of Physical Chemistry B, 2002, 106, 4470-4476.	1.2	28
230	Identification of Surfaceâ^'TiClxGroups on Silica by Raman Spectroscopy. Journal of Physical Chemistry B, 2002, 106, 6248-6250.	1.2	7
231	A Detailed Study of Thermal, Hydrothermal, and Mechanical Stabilities of a Wide Range of Surfactant Assembled Mesoporous Silicas. Chemistry of Materials, 2002, 14, 2317-2324.	3.2	325
232	Plugged hexagonal templated silica: a unique micro- and mesoporous composite material with internal silica nanocapsulesElectronic supplementary information (ESI) available: Fig. S1: X-ray diffractogram of a PHTS material. Fig. S2: TEM images of SBA-15 and PHTS-2. Fig. S3: hydrothermal stabilities. See http://www.rsc.org/suppdata/cc/b2/b201424f/. Chemical Communications, 2002, , 1010-1011.	2.2	168
233	Template extraction from porous clay heterostructures: Influence on the porosity and the hydrothermal stability of the materials. Physical Chemistry Chemical Physics, 2002, 4, 2818-2823.	1.3	34
234	Reproducible synthesis of high quality MCM-48 by extraction and recuperation of the gemini surfactant. Physical Chemistry Chemical Physics, 2001, 3, 127-131.	1.3	42

#	Article	IF	CITATIONS
235	Acidic porous clay heterostructures: study of their cation exchange capacity. Microporous and Mesoporous Materials, 2001, 49, 83-94.	2.2	46
236	Chemical modifications of oxide surfaces. Colloids and Surfaces A: Physicochemical and Engineering Aspects, 2001, 179, 145-150.	2.3	17
237	06-P-15 - Synthesis of mesoporous aluminosilicate FSM-materials derived from synthetic and natural saponite. Studies in Surface Science and Catalysis, 2001, , 201.	1.5	2
238	ALO _{X} -GRAFTED POROUS CLAY HETEROSTRUCTURES (PCH) WITH COMBINED MICRO- AND MESOPOROSITY. , 2000, , .		2
239	Silica-Pillared Clay Derivatives Using Aminopropyltriethoxysilane. Journal of Porous Materials, 2000, 7, 475-481.	1.3	17
240	Enhanced Brönsted acidity created upon Al-grafting of porous clay heterostructures via aluminium acetylacetonate adsorption. Physical Chemistry Chemical Physics, 2000, 2, 5750-5755.	1.3	64
241	MICROPOROUS PILLARED LAYERED MATERIALS FOR INORGANIC GAS AND ORGANIC VAPOR ADSORPTION. , 2000, , .		1
242	Title is missing!. Journal of Porous Materials, 1999, 6, 323-333.	1.3	6
243	Influence of water on the pillaring of montmorillonite with aminopropyltriethoxysilane. Physical Chemistry Chemical Physics, 1999, 1, 3703-3708.	1.3	14
244	Acid/base treatment of Al-PILC in KCl solution. Microporous and Mesoporous Materials, 1998, 26, 185-192.	2.2	13
245	Pillared Clays: Preparation, Characterization and Applications. , 1998, , 265-288.		33
246	Self-assembly of aluminium-pillared clay on a gold support. Journal of Materials Chemistry, 1997, 7, 443-448.	6.7	14
247	The relation between the synthesis of pillared clays and their resulting porosity. Applied Clay Science, 1997, 12, 43-60.	2.6	78
248	Title is missing!. Journal of Materials Science, 1997, 5, 83-94.	1.2	8
249	Preparation and characterization of zirconium pillared laponite and hectorite. Microporous Materials, 1996, 6, 27-36.	1.6	35
250	Theoretical evaluation of pillared clay adsorbents: Part II: Differences in porosity between Al-pillared laponite and hectorite. Journal of Porous Materials, 1996, 3, 157-168.	1.3	6
251	Theoretical evaluation of pillared clay adsorbents: Part I. The microporosity of Al- and Ti-pillared montmorillonite. Journal of Porous Materials, 1996, 3, 47-59.	1.3	19
252	Theoretical evaluation of pillared clay adsorbents: Part III: The total porosity and the macrostructure of Al-pillared montmorillonite and hectorite. Journal of Porous Materials, 1996, 3, 207-216.	1.3	6

#	Article	IF	CITATIONS
253	Theoretical evaluation of pillared clay adsorbents: Part IV: The microporosity of Fe- and mixed Fe-Zr-pillared montmorillonite. Journal of Porous Materials, 1996, 3, 217-225.	1.3	7
254	Physicochemical properties of ammonia-adsorbed alumina- pillared montmorillonite and structural aspects of the deammoniation process. Microporous Materials, 1994, 3, 149-158.	1.6	9